724U - Computational Engineering

Coursework 1:

FEM and Optimisation

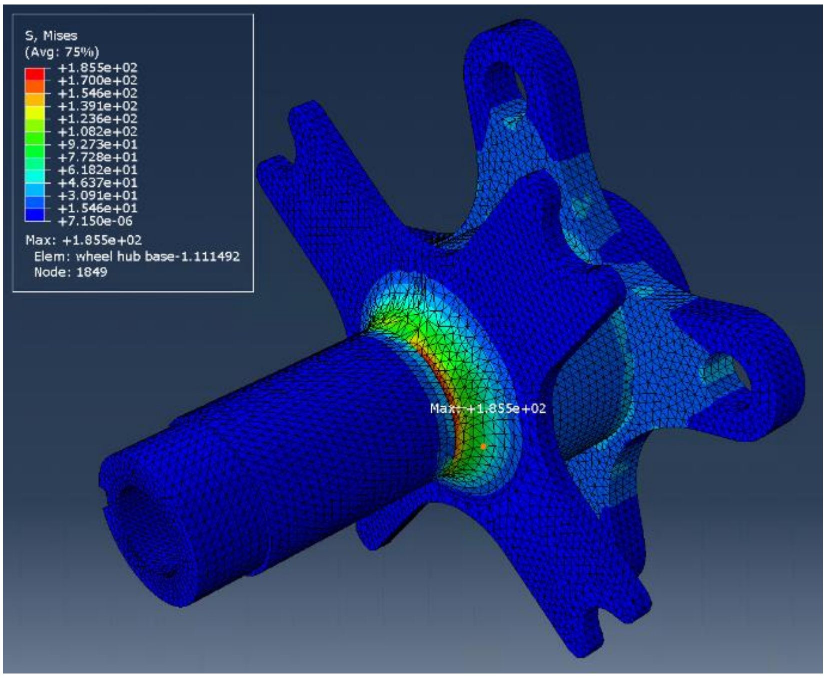

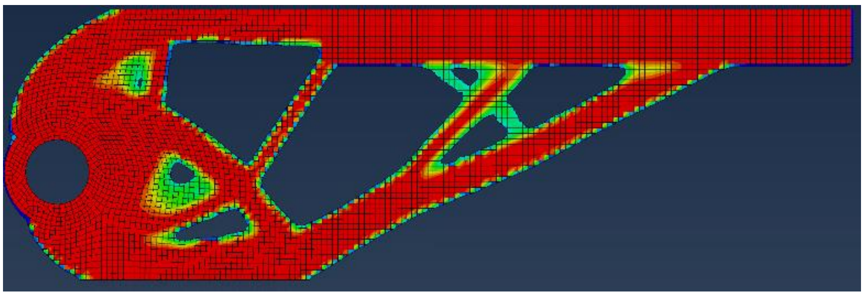

Student Name: Shannen Venethethan

Student ID: 210478226

December 2025

Finite Element Analysis Coursework: Part 1

Abstract:

This paper presents a Finite Element Analysis (FEA) of a 3D wheel hub modelled for the Queen Mary's formula student 2024 car. Geometry for the part was informed by these research papers [1,2,3,4] and adhered to the FSAE 2024 rulebook [5]. The part was simulated as aluminium 7075-T6 E= 7.17 x 10^4 MPa and v=0.33[3]. An encastre constraint was applied to shaft and a breaking moment of 347,000 Nmm was applied to the 4 bolt holes. Mesh convergence was run using h-refinement from 4mm down to 1.2mm element size, probed values were used to reach convergence at 1.6mm circa 200MPa with a variance of 2% between 1.2mm and 1. 6mm. Safety factor for the part at convergence value is 2.5. Quadratic element yielded convergence result but at an element size of 3mm. Larger fillet radii reduced local stress concentration.

Introduction:

Figure 1: CAD of wheel hub 3 views (a–c)

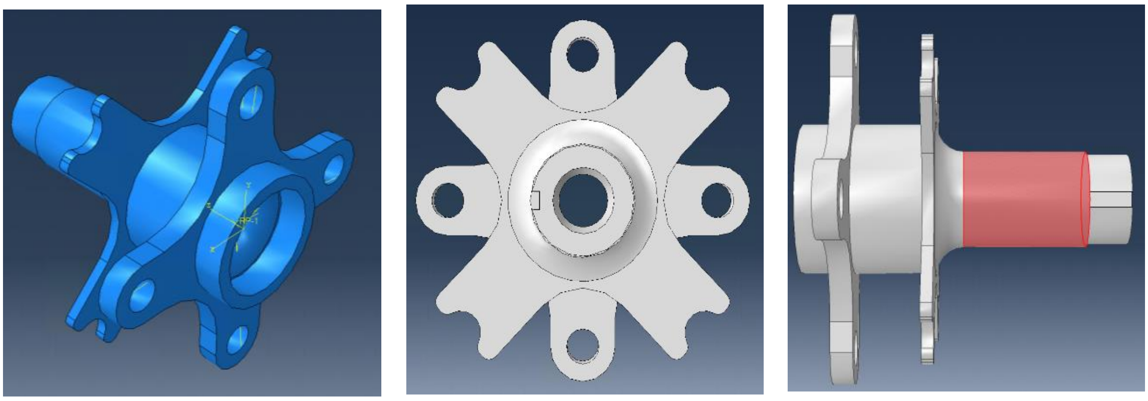

a b c

The wheel hub is a safety critical component that transfers the load from the tyre and torque from the breaks into the suspension while contributing heavily the unsprung mass of the car. In Formula student application hubs are typically lightweight and feature multiple complex geometries such as bearing seats bolt, patterns and fillets. These make it prone to local stress concentrations making it a suitable candidate for finite element analysis. Having analysis several papers [1,2,3,4] it can be noted that peak stress usually occurs near geometric discontinuities namely fillet, chamfers and bearing seat transitions.

This coursework analyses a 3D solid wheel hub Developed for the Queen Mary's University London Formula Student 2024 Car and is hance compliant with the FSAE 2024 rulebook [5]. The Wheel hub compromises of a bearing seat to the right of the red highlighted part in Fig 1c 30mm Diameter. A shaft of 32mm in diameter 70 mm in length highlighted in red Fig 1c. These is a part that connect to the disk brake which is 4mm thick and is made for 4 bolts 7mm in diameter Fig 1 b. The part that allows the wheel to be mounted with 4 bolts 10mm in diameter which is 8mm thickness Fig 1a. The shaft that connects to the break and wheel mount is 54 mm in diameter and 50mm in length Fig 1c. The material used for the wheel hub is Aluminium 7075-T6 which has Young's Modulus E= 7.17 x 10^4 MPa and Poisson's ratio v=0.33 [3].

The boundary conditions for the part were an encastre for region in red Fig 1c. and a moment force which was applied to reference point (RP1) in Fig 1a as it's the center of rotation for the part that hold the wheel. To allow for this force the reference point had interaction added between it and the surface inside where a wheel bolt would go. The moment force applied was 347,000 Nmm.

Results:

Mesh Convergence:

Figure 2: Probed stress and displacement against element size

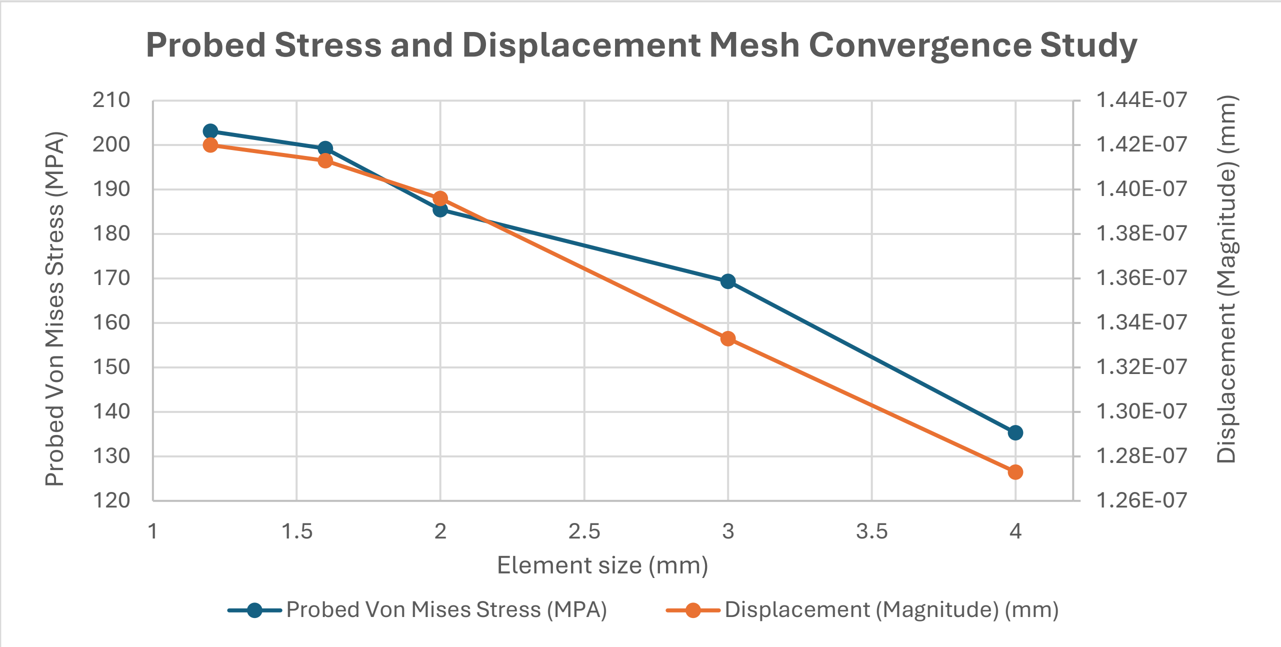

Figure 3: Von Mises stress for the 1.2 mm mesh highlighting the fillet hotspot**.**

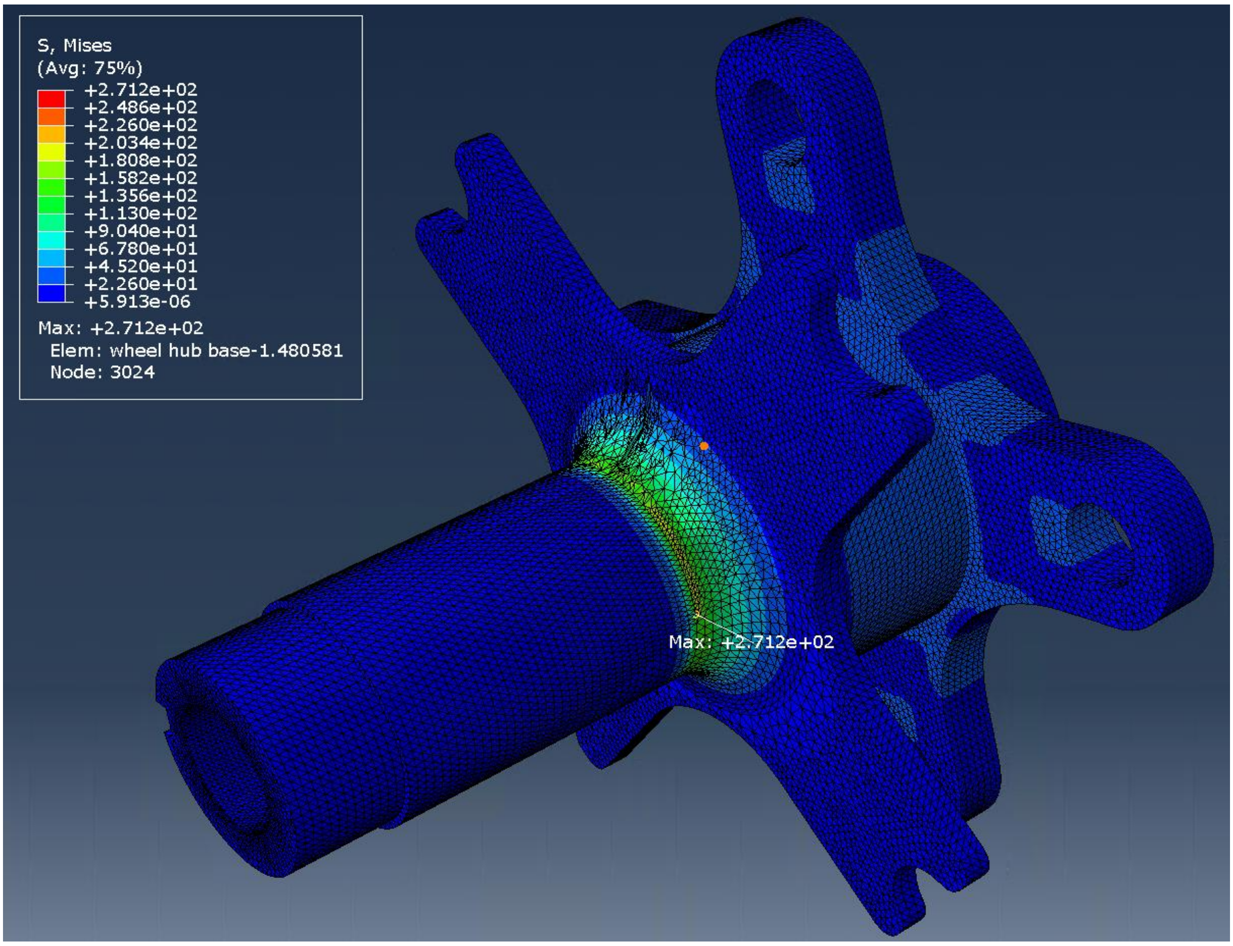

Finite element analysis is a numerical approximation for the parameters we are solving for; its accuracy is heavily dependent on the element size used to analyse the model. A mesh convergence study was therefore conducted to verify that the final simulation data was independent of the element size used. This means the solution found is numerically stable and is not using excess computational resources to achieve a similar result. This iterative process requires increasing the resolution of the mesh and comparing key result parameters until successive runs yield results that fall within a reasonable margin of error, usually 5%.

For this study Von Mises stress was the primary metric being observed. Displacement magnitude was also monitored against the element size, which was the independent variable in the study following the standard h-refinement technique. The element size was reduced in increments from 4mm to 1.2mm (4,3,2,1.6,1.2) meaning the number of elements went from 28,482 to 775,019. The final two meshes are not of the uniform ratio as the previous three as anything beyond 1.2mm ran into student limitation and yielded errors.

A key consideration when evaluating the Von mises stress calculated by Abaqus is the location of the absolute maximum stress. This usually happens in close vicinity to the encastre boundary condition Fig.3. Given the region is fully fixed in place it can produce an artificial local hotspot. With finer mesh sizes this hotspot may increase in von mises stress value and make the global stress appear as if it has not converged when the opposite is true. Hance making raw maximum stress unrepresentative of the component response meaning it cannot be used in the convergence study.

Convergence was assessed using a consistent probed Von Mises stress value, taken away from the fixed boundary condition in the representative stress field. Displacement Magnitude was however taken at the location of maximum deflection as it was in the same general location (In plane with RP1 Fig. 1a at the extremity of that geometry) and converged without needing to probe.

The probed stress values and displacement trends with element size Fig.2. We can see as the as the mesh get finer probed Von Mises stress values increase linearly 135.3 Mpa (4mm) to 185.5 MPa (2mm), before reaching the asymptote as 199.2 MPa (1.6mm) and 203.1MPa (1.2mm). The last two results are within 2% of each other satisfying the typical 5% tolerance. The same is true for displacement (magnitude) converging at 1.6mm.

Regarding unprobed values which are in the Table 3 in the Appendix. Maximum stress was 221.5 MPa (1.6mm) and 271.2 MPa (1.2mm) which further accentuates their sensitivity to local constraint hotspot. Making probed value the correct solution.

Safety factor for the part is calculated using:

Equation 1: Factor of safety

$$FoS = \frac{\sigma_y}{\sigma_{vm}}$$

$$FoS = \frac{503}{203.1} = 2.5$$

Using the 1.2mm value we have $\sigma_{vm} = 203.1$ MPa and yield stress of $\sigma_y = 503$ MPa giving a safety factor of 2.5 which makes the part suitable for the application.

Element type:

Figure 4: Linear vs quadratic bar charts (a) Von Mises stress (b) Displacement

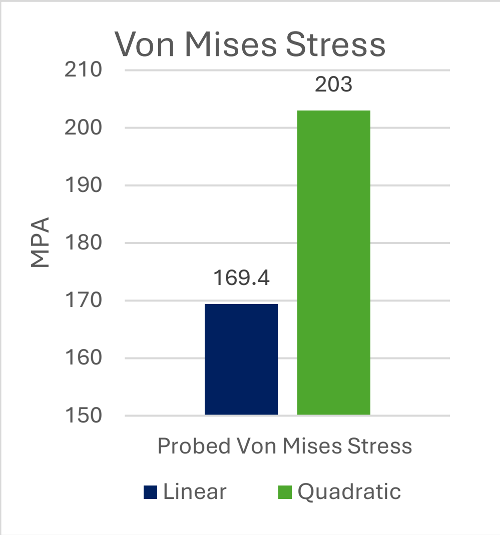

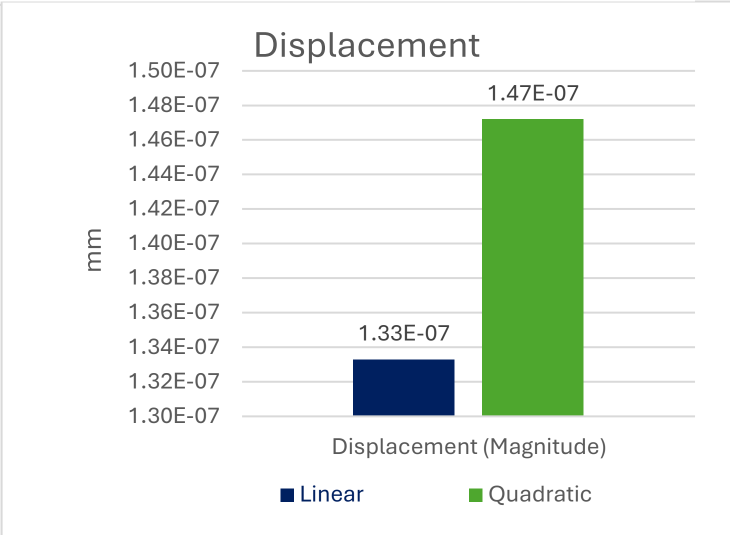

To assess the difference between linear and quadratic formulations under the same load and boundary conditions. A study was conducted at a fixed element size of 3mm (2mm was not viable due to licence limitations). The results from this study are shown in Fig. 4 a & b. The linear model estimated the Von Mises stress at 169.4 MPa and a displacement of 1.33 x 10^{-7}mm whereas the quadratic model estimates 203 MPa and a displacement of 1.47 x 10^{-7}mm. The higher values are expected as higher order elements provide improved strain interpolation and reduced artificial numerical stiffness. This allows for steeper stress gradients near the fillet to be captured with more accuracy. The highlight of this study is that at 3mm element size we reach Von Mises stress and displacement results which are concordant with the convergence in Fig.2 which was only achieved with the finest mesh of 1.2 mm. This indicated that quadratic elements could achieve comparable accuracy with coarse mesh sizes which is beneficial when computational efficiency is required.

Additional design iteration study (Fillet radius):

Figure 5: CAD of wheel hub with fillet region highlighted

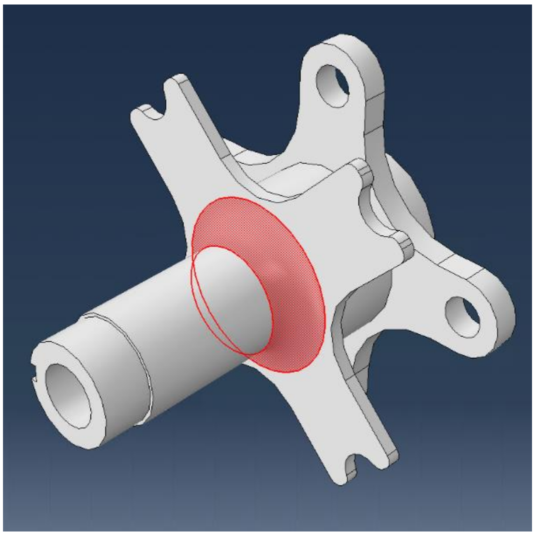

Figure 6: Stress and Displacement against fillet radius

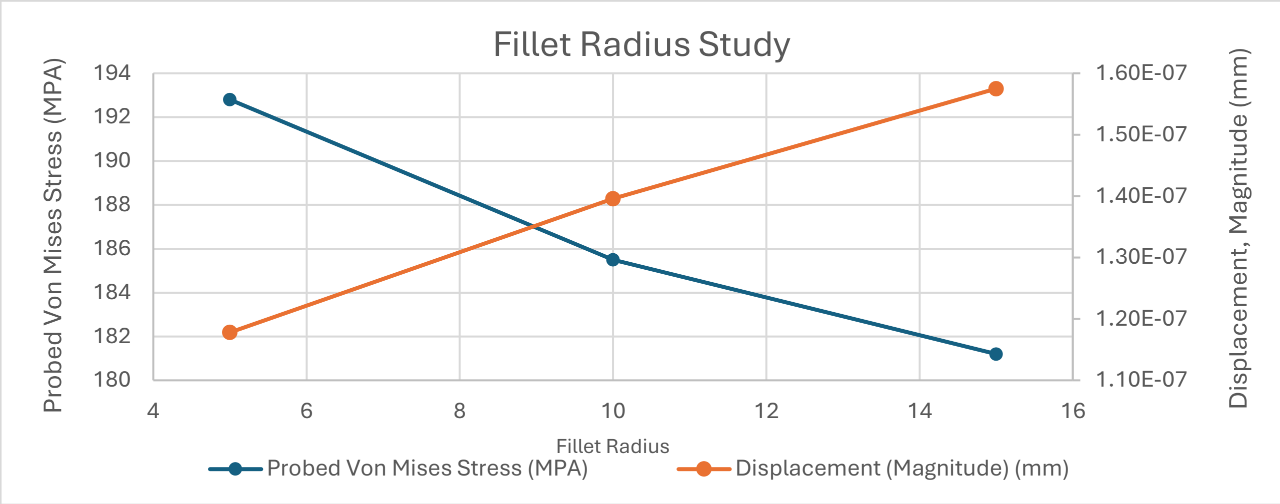

From the previous studies global stress contours it can be noted that there is a critical hotspot at in the fillet highlighted in Fig. 5. To reduce this stress concentration a short sensitivity study was performed by analysing the effect of reducing it (5mm) and increasing it (15mm). All force and boundary condition remained the same and it was tested using linear elements with element size of 2 mm. It can be observed from Fig. 6 there is a clear trend that as radii increases the probed Von Mises stress value decreases with the lowest being achieved of 181.2 MPa on the 15mm radii.

Although not explicitly required in the updated brief, this additional sensitivity check was included to demonstrate how the identified stress concentration can be mitigated through a simple geometric modification

Conclusions

This coursework used finite element analysis (FEA) to simulate the stress and displacement response of a 2024 Formula student wheel hub manufactured from aluminium 7075-T6 which has Young's Modulus E= 7.17 x 10^4 MPa and Poisson's ratio v=0.33 [3]. The part was bound by the shaft highlighted in Fig 1c using the encastre function and moment of 347,000 Nmm was applied to RP1 Fig 1a to simulate breaking force. From initial result it is clear that there is a localised hotspot at the boundary between the fillet and fixed geometry.

A mesh convergence study was then run using elements size from 4 mm to 1.2mm using the conventional h-refinement method. Given that the absolute maximum value was given but the localised hotspot the only solution to find convergences was to use probed values way from the fixed boundary. The values converged to the asymptote Fig. 2 and converged to a value of approximately 200 MPa at 1.6mm mesh size as the difference between 1.2mm (203.1 MPa) and 1.6mm (199.2 MPa) is only 2% which is within the typical 5% tolerance. In contrast the maximum stress values are 1.2mm (271.2 MPa) and 1.6mm (221.5 MPa) confirming they are not representative for convergence. A suitable safety factor of approximately 2.5 was also calculated.

Element formulation was tested at 3mm element size. The quadratic element predicted 203 MPa which closely matches the linear 1.2mm (203.1 MPa) but at a significant higher computational efficiency.

Finally, to a short study was conducted and yielded that higher radii fillet reduced local stress concentration. Future work would include simplifying geometry to allow for hex dominated meshing and testing against Tet.

Optimisation Coursework via Abaqus: Part 2

Introduction:

Figure 7: Bicycle brake handle geometry

Part B investigated the topology optimization for a 2D bicycle brake handle using Abaqus [6] built in Density based SIMP model. The objective of the study was to minimise volume which maintaining stiffness in the part. To achieve this the problem was set up as a compliance minimization with the independent variable being Volume Fraction (VF) of the area highlighted in red Fig.7.

The geometry of the domain started from a 180 mm x 50mm rectangle. An 8 mm hole centred 20 mm in both positive x and y direction from the bottom right corner was made. To ensure it would end up as a bicycle handle, the part was further partitioned with a 100mm x 10 mm rectangle placed 10mm in the negative x direction from the top corner. A circle of 10mm centred with the hole was also placed leaving the red region used for the optimization. The part is 15mm in thickness. The pressure of 0.067 MPa was place as shown as in Fig.7 this was calculated using F = pLt using a force of 100N. Finally, an encastre parameter was applied to the 10 mm circle as is the pivot.

The optimization study was run for VF 10% to 40% in increments of 10% and a mesh sensitivity study was also performed using VF 30% using mesh of 20x20 50x50 and finally 100x100. The part was simulated in Aluminium 6061-T6 E= 6.9 x 10^4 MPa and v=0.33.

Results:

VF Analysis:

Figure 8: (a) Legend (b) VF 10 (c) VF 20 (d) VF 30 (e) VF 40

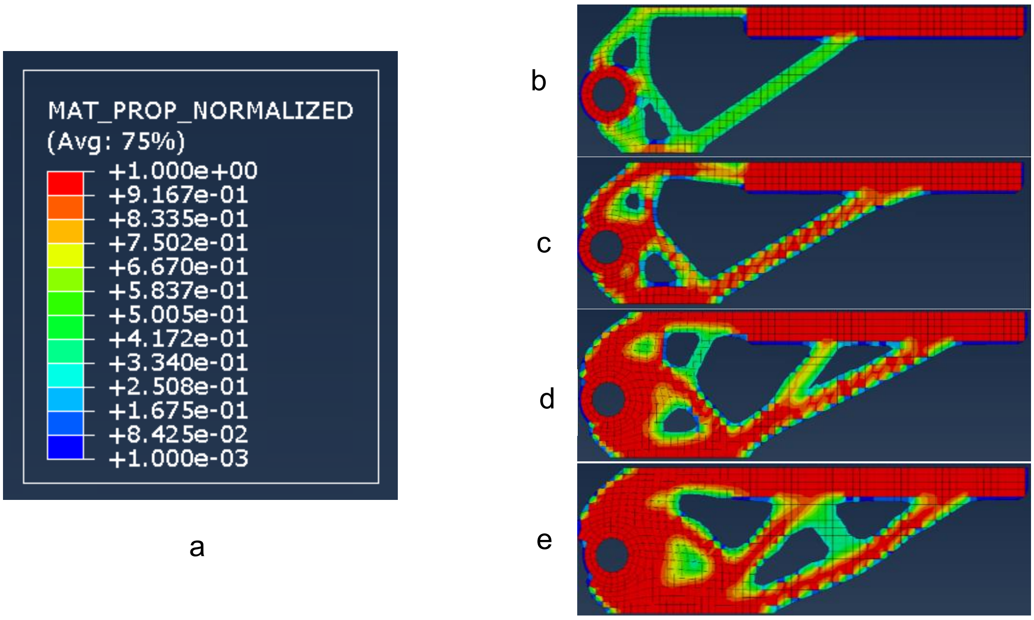

Fig. 8a shows the optimised material distribution as a variable MAT_PROP_NORMALIZED which shades retained material in red and removed material in blue. At VF 10% Fig 8b the solution collapses into a diagonal and horizontal thin stuts linking the pivot region to the loaded region.

This solution has the maximum mass reduction however it would have also the lowest safety factor making it unsuitable for manufacturing. At VF 20% we can observe both struts become thicker. At VF 30% additional triangulation appear near the mid span cut out and around the pivot this improves stiffness. At VF 40% the topology remains largely unchanged with only the thickening of the struts being noticeable which indicates diminishing returns in mass saving.

Mesh resolution:

Figure 9: (a) Legend (b) Coarse mesh 20x20 (c) Medium mesh 50x50 (d) Fine mesh 100x100

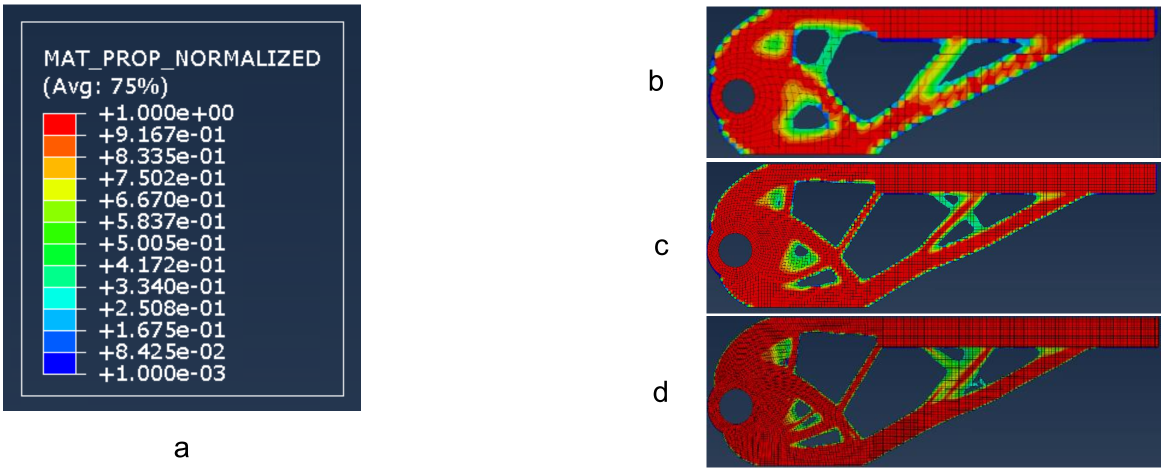

For the mesh sensitivity study, which was conducted at VF 30%, three quad structure mesh were compared: coarse 20x20, medium 50x50 and fine 100x100. The target element size was dictated by the shortest edge e.g. 20x20 had an element size of 2.5mm as the shortest edge is 50mm.

At 20x20 Fig. 9b the mesh produces a blocky material layout and a smeared void boundary. At 50x50 Fig. 9c the naib load paths become clear and secondary cut outs stabilise. At 100x100 Fig 9d the mesh boundaries are extremely sharp revealing finer topology, this however come at a high computational cost and increased risk of minuscule non manufacturable features.

Conclusion:

This optimization study applied Abaqus' [6] density based SIMP topology optimization method to a 2D bicycle brake handle. Two studies were conducted one optimising the structure based on an independently set volume factor (VF) while minimizing compliance (maximise stiffness). The other maintain a constant VF but increasing the mesh resolution.

The VF analysis yielded increasingly better result from VF 10% up to a VF 30% which had clear detailed load paths and triangle structures to distribute the load more evenly. At VF 40% The additional material was not used effectively. VF 30% the best stiffness to volume balance.

Comparing mesh size at VF 30%, 20x20 mesh produced blocky members and smeared void boundaries. 50x50 yielded much sharper boundaries and more efficient topology. 100x100 was more computationally intense and produced small unmanufacturable geometries. Making 50x50 the most suitable mesh tested.

Future work would include running VF 20, VF 25 and VF 30 simulation with meshes between 50x50 and 100x100 to create a more optimised part.

For industrial manufacture the most optimised solution for the design constraint such as weight and /or cost would be interpreted into CAD with parametrised dimensions. This would the be used to manufacture the part

Additional Optimisation Coursework via Python: Part 3

Results:

Filter radius study:

Figure 10: Filter radius study (a) rmin = 0.5 (b) rmin = 2 (c) rmin = 5

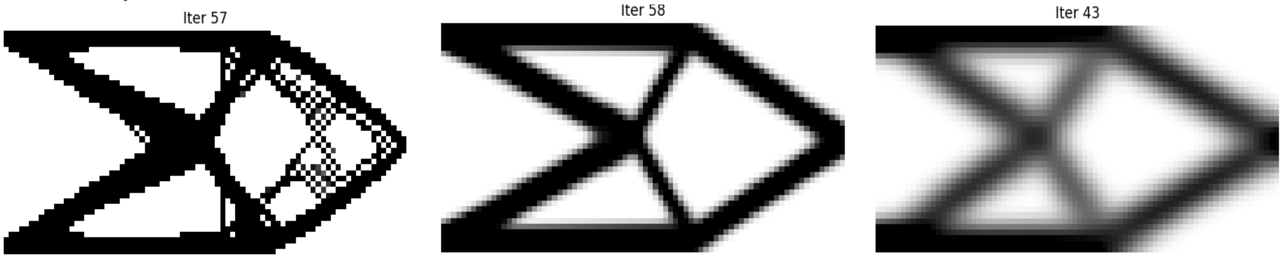

a b c

A filter radius sweep was performed to observe how regularisation affected SIMP mode. r_{min} of 0.5,2 and 5 was tested. For r_{min}=0.5 Fig 10a we can observe strong checkerboarding and pixel level oscillations. Increasing to r_{min}=2 Fig 10b gives a cleaner more continuous truss structure. Finally, at r_{min}=5 Fig 10c the topology is heavily smoothed and lack detail.

Mesh resolution study:

Figure 11: Mesh resolution study (a) 40x20 (b) 80x40 (c) 120x60

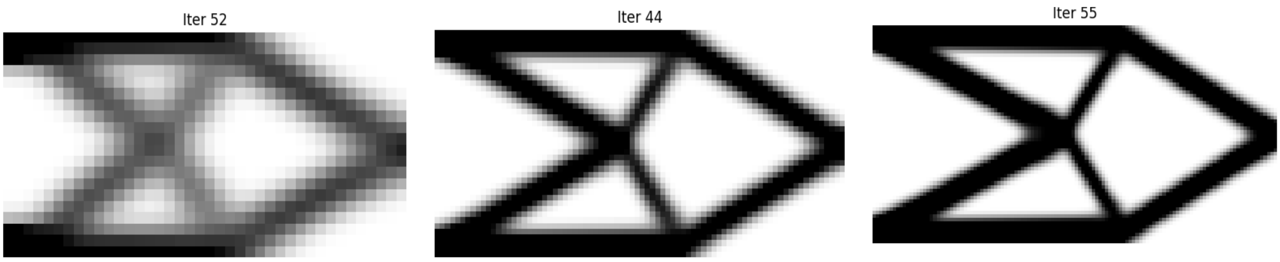

a b c

A mesh resolution analysis was carried out at a constant volume fraction and filter setting r_{min}=3.

The coarse mesh 40x20 Fig 11a produces blurry and blocky boundaries making features hard to distinguish. The medium mesh 80x40 Fig 11b is a considerable improvement as the load path can be easily identified. The fine mesh 120x60 Fig 11c produces the highest geometric fidelity with the only caveat being computational cost.

Discussion:

Analysing both studies, we can observe that there is a strong trade-off between numerical stability, feature resolution and runtime. We can draw that increasing r_{min} yield stronger sensitivity filtering leading to suppressed high frequency density oscillations and reducing checkerboarding. This improves interpretability and manufacturability however increasing it too high eg. r_{min}=5 Fig 10c provides an overly smoothed structure and can remove secondary struts necessary for load bearing. In the Mesh density study, the variable mainly changes the geometric fidelity of the output. Lower resolution meshes can omit thinner structures. While the quality of the output increases with mesh resolution it scales with computational cost, the fine mesh took 7 times longer than the coarse mesh Table 5. In conclusion a moderate approach to both filters yields the most efficient output hance r_{min}=5 and resolution of 80x40.

References:

1. Shinde T, Chavan R, Savadekar P, Shinde D, Jagtap N. Failure Analysis of a Wheel Hub of Formula Student Racing Car. Journal of The Institution of Engineers (India): Series D. 2021 Jan 6;102(1):73–8.

2. Óskar Kúld Pétursson 1989. Uprights, wheel hubs and brake system for a new Formula Student race car [Internet]. Skemman.is. 2019 [cited 2025 Dec 15]. Available from: https://skemman.is/handle/1946/26682

3. Gowtham V, Ranganathan AS, Satish S, John Alexis S, Siva kumar S. Fatigue based design and analysis of wheel hub for Student formula car by Simulation Approach. IOP Conference Series: Materials Science and Engineering. 2016 Sep;149:012128.

4. Rincón García, Jesús. Analysis of Wheel Hubs : Student Car. Theseusfi [Internet]. 2025 [cited 2025 Dec 15]; Available from: https://www.theseus.fi/handle/10024/75036

5. Formula SAE Rules 2024 [Internet]. Fsaeonline.com. 2023. Available from: https://www.fsaeonline.com/cdsweb/gen/DownloadDocument.aspx?DocumentID=369d01c0-589d-4ebe-b8d4-b07544f4a52b

6. Abaqus. Abaqus [Internet]. Dassault Systèmes. 2023. Available from: https://www.3ds.com/products/simulia/abaqus

Appendix:

Table 1: Part 1 raw convergence data convergence analysis

Element size (mm)	Number of elements	Probed Von Mises Stress (MPA)	MAX not probed	Displacement (Magnitude) (mm)
1.2	775019	203.1	271.2	1.42E-07
1.6	347021	199.2	221.5	1.41E-07
2	184009	185.5	N/A	1.40E-07
3	60109	169.4	N/A	1.33E-07
4	28482	135.3	N/A	1.27E-07

Table 2: Part 1 raw element type data

Element type	Element size [mm]	Number of elements	Probed Von Mises Stress	max not probed	Displacement (Magnitude)
Linear	3	60109	169.4		1.33E-07
Quadratic	3	60109	203	214	1.47E-07

Table 3: Part 1 raw fillet radii data

Filet radius	Element size [mm]	Number of elements	Probed Von Mises Stress (MPA)	Max Stress not probed	Displacement, Magnitude (mm)
5	2	183446	192.8	N/A	1.18E-07
10	2	184009	185.5	N/A	1.40E-07
15	2	189550	181.2	214.4	1.58E-07

Figure 12: Part 1 Displacement gradient front view element size 2mm

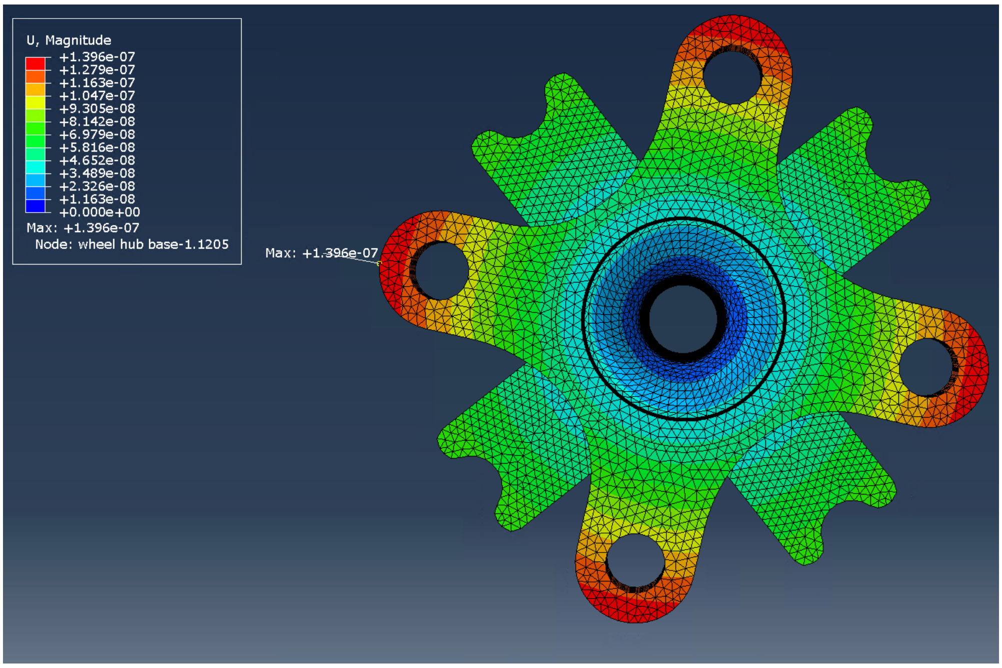

Table 4: Part 3 Filter radius study raw runtime data

rmin	run time (s)	Nº iteration (convergence)
0.5	19.1	57
2	29.1	58
5	40.2	43

Table 5: Part 3 Mesh resolution study raw runtime data

mesh size	run time (s)	Nº iteration (convergence)
40x20	10.9	52
80x40	26.1	44
120x60	70.6	55